STUDY OF CRACK ONSET AT HOLES IN PMMA. DIFFICULTIES IN CHARACTERIZING THE MATERIAL

A. Leite [1,2], V. Mantič [1], F. París [1]

[1] Grupo de Elasticidad y Resistencia de Materiales, E.T.S. de Ingenieros
Universidad de Sevilla, Camino de los Descubrimientos s/n
E-41092 Sevilla, España
E-mail: mantic@esi.us.es, paris@esi.us.es

[2] Departamento de Engenharia Mecânica
Instituto Superior de Engenharia de Lisboa
Rua Conselheiro Emídio Navarro,1, 1959-007 Lisboa, Portugal
E-mail: leite@dem.isel.ipl.pt

ABSTRACT

There is still not full confidence in the capability of the actual failure criteria for composites to predict satisfactorily either the onset of the damage in form of cracks or the crack propagation in these materials. Finite Fracture Mechanics (FFM) introduces a new approach to characterize crack onset and may afford a new insight into the analysis of the failure mechanisms in composites. In the present initial work, FFM concepts are applied to characterize damage in a simple configuration, comparing semianalytical predictions with the experimental results obtained. A rectangular plate with a central hole subjected to uniaxial tension at the outer boundary is studied with the objective to elucidate the size effect in failure load, by testing for several hole diameters. The plate material is polymethyl metacrylate (PMMA). The influence of testing parameters such as test velocity on the material characterization is also studied and discussed.

KEY WORDS: crack initiation, stress concentration, Finite Fracture Mechanics, PMMA, composites.

1. INTRODUCTION

Although the Composite Materials applications in the aeronautical industry have considerably increased in recent years, there is still not full confidence in the capability of the actual failure criteria for composites to predict satisfactorily either the onset of the damage in form of cracks or the crack propagation in these materials. New micro- and meso-mechanical studies are required to understand in depth the failure mechanisms in composite materials. Finite Fracture Mechanics (FFM) [1] introduces a new approach to characterize crack onset and may afford a new insight into the analysis of these failure mechanisms. As an ultimate objective of this work, the authors want to apply this formulation to study theoretically and experimentally the onset and propagation of a crack in composite materials on micro-level, namely the problem of the fiber-matrix debonding [2].

In order to achieve an in-depth understanding of the crack onset phenomena, such an analysis is first carried out by applying the FFM concepts to a simple configuration of a plate with a central hole subjected to uniaxial tension at the outer boundary [3], shown in Figure 1. This is used to elucidate the size effects in failure load by testing for several hole diameters. Thus, one of the objectives of this initial work is to clarify the role of parameters that control the appearance of damage and its initial growth in originally undamaged specimens.

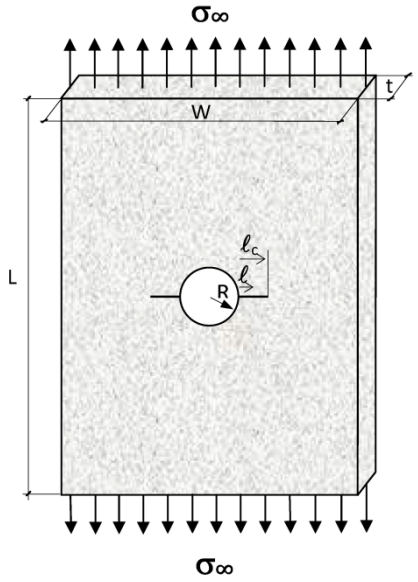

Figure 1. Geometry of the plate with hole and emanating cracks.

The plate height is denoted by L; the width by W, the thickness by t, the hole radius by R, the emanating cracks length at onset by ℓ_c, the intermediate crack lengths by ℓ, the applied remote tension by σ^∞ and the critical remote tension causing the crack onset by σ_c^∞.

The failure criterion proposed is explained in Section 2. The carried out experimental program is described in Section 3, including in the first parts the specimen preparation, the determination of tensile and fracture properties of the material used (polymethyl metacrylate, PMMA), and also observed difficulties. In the last part of this section, the study of crack onset at a hole is presented. First, specimen fabrication and testing are discussed, and then the test results are presented and compared with the FFM predictions. Finally, a discussion of the obtained results and conclusions are given.

2. FAILURE CRITERIA

2.1. Tensile stress criterion

The tensile stress criterion assumes the existence of a critical tension σ_c (material tensile strength), and uses the well known Kirsch's expression for stresses along the symmetry axis of the infinite plate with a circular hole perpendicular to the load. Then, in view of the notation introduced in Figure 1, and assuming that two cracks of the length ℓ_c will abruptly initiate at the hole boundary in the direction perpendicular to the load, the remote critical stress σ_c^∞, should accomplish the following inequality:

$$\sigma_c \le \frac{\sigma_c^\infty}{2}\left(2+\frac{R^2}{(R+\ell)^2}+3\frac{R^4}{(R+\ell)^4}\right),\ \ 0 \le \ell \le \ell_c \qquad (1)$$

2.2. Incremental energy criterion

The following inequality represents the necessary energetic condition for the onset of a crack of the finite length ℓ_c:

$$\int_0^{\ell_c} G(\ell)t\,d\ell \ge G_c t \ell_c \qquad (2)$$

The energy released during the crack abrupt onset is given by the integral of G (Energy Release Rate, ERR) on the left-hand side of this inequality, whereas the energy required for this crack onset is given by the expressions on its right-hand side, where G_c. is the critical energy release rate.

The stress intensity factor in fracture Mode I, K_I, for two cracks of the length ℓ emanating from a hole, is given by the well known Newman's expression:

$$K_I = \sigma^\infty\sqrt{\pi\ell}\left(1+0.5\frac{R}{R+\ell}\right)\left[1+1.243\left(\frac{R}{R+\ell}\right)^3\right] \qquad (3)$$

Then, the well-known Irwin's relation between the ERR, G, Young Modulus, E, and K_I,

$$G=\frac{{K_I}^2}{E'} \qquad E'=\begin{cases}E & \text{Plane Stress}\\ \frac{E}{(1+\nu^2)} & \text{Plane Strain}\end{cases} \qquad (4)$$

can be substituted into inequality (2).

2.3. Coupled stress and energy criterion

Taking into account that tensions are decreasing with the distance from the hole, the stress criterion (1) leads to the following condition for the critical crack length ℓ_c and the critical remote load σ_c^∞:

$$\sigma_c^\infty = \frac{2\sigma_c}{\left(2+\frac{R^2}{(R+\ell_c)^2}+3\frac{R^4}{(R+\ell_c)^4}\right)} \qquad (5)$$

Due to the dependence of G on the square of K_I, and consequently on the square of σ^∞, and taking into account that G is increasing with ℓ, the energy criterion (2) leads to another condition for the critical crack length ℓ_c and the critical remote load σ_c^∞:

$$(\sigma_c^\infty)^2\int_0^{\ell_c}\hat{G}(\ell)d\ell = G_c\ell_c \qquad (6)$$

where $G=(\sigma^\infty)^2\hat{G}$. By considering a coupled criterion defined by conditions (5) and (6), we obtain the system of two nonlinear equations for two unknowns σ_c^∞ and ℓ_c. Eliminating σ_c^∞ from the system we arrive to the following nonlinear equation for the unknown ℓ_c:

$$\left(\frac{2\sigma_c}{\left(2+\frac{R^2}{(R+\ell_c)^2}+3\frac{R^4}{(R+\ell_c)^4}\right)}\right)^2\int_0^{\ell_c}\hat{G}(\ell)d\ell - G_c\ell_c = 0 \qquad (7)$$

This equation can be solved numerically, for example using *Mathematica* package. Once the value of ℓ_c is computed, the corresponding value of σ_c^∞ is easily obtained from equation (5).

3. EXPERIMENTAL PROGRAM

3.1. Tensile Properties

The plate material is polymethyl metacrylate (PMMA). In order to define PMMA elastic properties, we have used standard ASTM D638-03 [4] as guideline.

If the specimen thickness is less than 7 mm type I specimen geometry should be used, as shown in Figure 2. If it is higher than this value type III should be used. The basic difference in these types is the width (and consequently other dimensions). The width for type I is 13 mm and for type III is 19 mm.

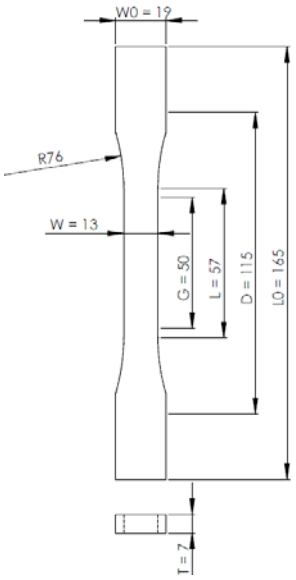

Figure 2. Tension specimen (type I - ASTM D638-03).

The plate of PMMA used to fabricate the specimens had an average maximum thickness of 7 mm. Thus, five specimens of type I were manufactured. In each specimen bidirectional strain gages (one in the longitudinal and the other in transversal direction) were glued to test for the Young modulus, Poisson coefficient and ultimate failure load. Although the standard defines as mandatory to test PMMA at 5 mm/min, this first batch was tested at the velocity of 0.5 mm/min in a electromechanical INSTROM test machine with load cell of 100 kN, equipped with an extensometer. The specimen mounted in the machine is shown in Figure 3.

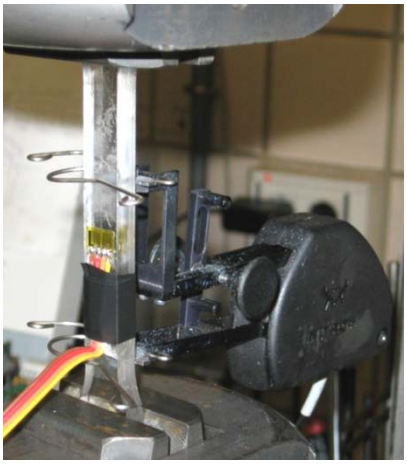

Figure 3. Tension test specimens (type I).

The test results obtained using this velocity are presented in Table 1. The specimens after rupture are shown in Figure 4. The average value of the ultimate failure load was, without taken into account the coupon number 3, σ_c=33.8 MPa.

The stress-strain curves obtained using the longitudinal strain gages, are shown in Figure 5.

Table 1. Test results for tensile specimens type I, tested with 0.5 mm/min.

Spec. No.	Rupture Load [N]	Area [mm^2]	σ_c [MPa]	Observation
1	2557.5	91	28.1	
2	3936.8	91	43.3	
3	2185.7	91	24.0	Broken out of the test length
4	2849.8	91	31.3	
5	2970.5	91	32.6	

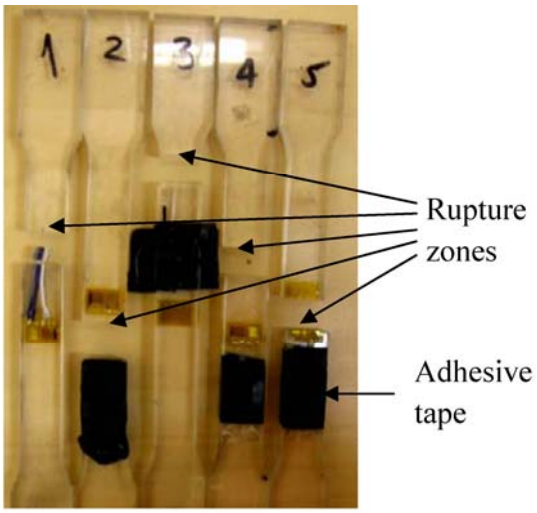

Figure 4. Tension test specimens (type I). Tested at 0.5 mm/min.

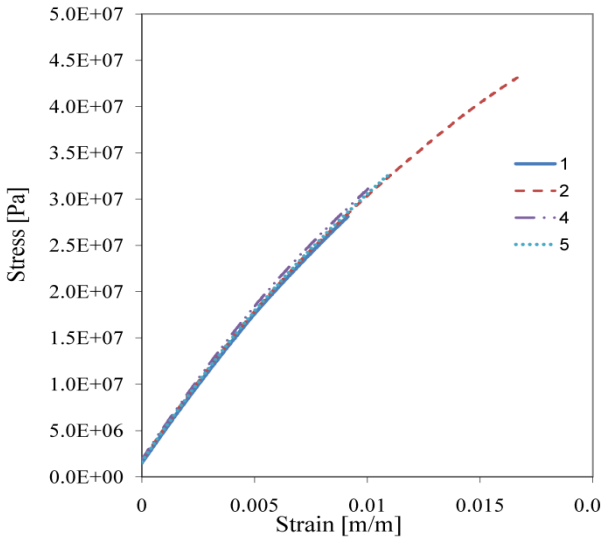

Figure 5. Stress-strain curves obtained from specimens (type I - ASTM D638-03). Tested at 0.5 mm/min.

One can see from Figure 5 that the linear elastic approximation is reasonable for this material. It is also

possible to observe its brittle fracture. The calculated average Young modulus was E=2.85 GPa, and Poisson ratio ν=0.34. These values are within the published PMMA properties, but the ultimate stress σ_c=33.8 MPa seemed to be too much low (less than half of the usual).

Thus, new five, type I, coupons were fabricated and tested now at 5 mm/min velocity (without strain gages). All the specimens broke at the filleted machined parts, invalidating the results. These led us to the decision to manufacture straight specimens (without tabs and strain gages). The results were surprising: the average ultimate stress was more than double (σ_c=73.15 MPa) as shown in Table 2.

Table 2. Test results for straight tensile specimens of type I, tested with 5 mm/min.

Spec. Nr.	Rupture Load [N]	Area [mm^2]	σ_c [MPa]
1	6273.32	84.8	74.4
2	6130.87	82.9	74.0
3	6335.41	87.0	72.8
4	6324.02	87.0	72.6
5	6230.8	86.1	72.3

To see if there were any difference due the change from type I to III, as the specimen thickness was on the limit between the two types, three specimens with 7.05 mm thickness were tested and the results are shown in Table 3, with an average of σ_c=72.7 MPa.

Table 3. Test results for straight tensile specimens of type III, tested with 5 mm/min.

Spec. Nr.	Rupture Load [N]	Area [mm^2]	σ_c [MPa]
1	9974	136.1	73.3
2	9956	136.1	73.2
3	9721	135.7	71.6

3.2. Fracture Properties

To obtain fracture toughness one can use the standard ASTM D5045-07 [5] to design Compact Tension (CT) specimens. In plastics, in general, the main difference to metals in fracture testing is that the natural initial crack cannot be easily made by fatigue cycling, due to the fragility of the specimen. Thus the standard advises making the natural crack by tapping a fresh razor blade into the specimen (with a hammer for example) or if this is not possible, by sliding with the blade into the machined notch. The usual dimensions of CT for our case are B=7 mm; W=4B=28 mm and a=14 mm (machined notch plus natural crack).

To fix the razor blade vertically in order to hammer it against the CT coupon, a jig was necessary. After some research [6-7] that involved hammering, pressing, and drop of a dead weight, the option to tapping our jig with the hammer [6] was taken, as shown in Figure 6. As justified by [6] and other authors, obtaining the natural crack by fatigue, sliding or pressing a razor blade gives higher stress intensity factors, which can induce in erroneous fracture properties.

First nine CT coupons were made using tapping, but that task was not easy because the blade usually collapsed by buckling, as can been seen in Figure 7.

Figure 6. Razor blade support device and application into CT-fracture specimen.

Figure 7. Razor blade damaged after tapping operation.

Then other blades, thicker than the initial razor blades, were adopted, and the crack generation was successful, as shown in Figure 8.

Figure 8. CT-fracture specimen with a successfully obtained natural crack.

To date it was not possible to test for fracture toughness because of necessity of carefully mounted CMOD strain gage and a sufficiently small load cell for such a small CT specimen not available in our laboratory. In virtue of lack of time, we have decided to use three representative values for the range of K_{Ic} for PMMA from [8].

3.3. Crack onset at holes

To study the crack onset in holes, coupons with 300 mm long and 50 mm width with different hole sizes were machined. The hole diameters made were 10, 5, 3, 2, 1 and 0.5 mm. Initially five coupons for each group of diameters were fabricated, but after several machining and testing difficulties, like rupture in the filleted zones, as seen in Figure 9, only four successfully tested coupons for each group have been achieved. Some of the specimens were fabricated as straight with 40 mm width (without fillets). The test velocity was 0.5 mm/min because these tests were initiated before the second and third batches of tensile tests. The test results are shown in Table 4.

Table 4. Test results for plates with holes.

Speci-men	Max Load	Width	Thick-ness	$\sigma_c^\infty / \sigma_c$	
Ø-Nr.	[kN]	[mm]	[mm]	σ_c = 33.8 [MPa]	σ_c = 73.15 [MPa]
10-1	11.3	49.93	6.88	0.98	0.45
10-2	11.3	49.98	6.85	0.98	0.45
10-3	11.0	50.03	7.04	0.92	0.43
10-4	11.6	49.90	7.00	0.98	0.45
5-1	14.0	49.95	6.93	1.19	0.55
5-2	13.9	50.03	6.76	1.22	0.56
5-3	14.3	50.19	7.11	1.18	0.55
5-4	14.1	50.07	7.08	1.17	0.54
3-1	14.3	50.02	7.08	1.19	0.55
3-2	13.8	49.98	6.81	1.20	0.56
3-3	11.2	49.91	6.30	1.05	0.49
3-4	14.7	49.54	6.15	1.42	0.66
2-1	11.5	40.40	6.22	1.35	0.62
2-2	11.8	40.75	6.34	1.35	0.62
2-3	11.1	40.70	6.15	1.31	0.61
2-4	11.9	40.29	6.22	1.41	0.65
1-1	11.6	39.89	6.38	1.34	0.62
1-2	13.1	40.12	6.17	1.56	0.72
1-3	12.6	40.44	6.18	1.49	0.69
1-4	12.1	40.50	6.13	1.44	0.66
0.5-1	14.4	40.10	6.48	1.64	0.76
0.5-2	14.4	40.13	6.54	1.62	0.75
0.5-3	14.3	39.85	6.79	1.56	0.72
0.5-4	16.1	40.03	7.27	1.63	0.75

Figure 10 shows the rupture for the case of a 5 mm hole. All the ruptures were instantaneous.

Figure 9. Plate with 3 mm diameter hole, after rupture near the filleted zone (and not at the hole).

Figure 10. Plate with 5 mm diameter hole, after rupture.

In Figure 11 a rupture in a 0.5 mm hole is shown, that-produced a vertical crack that can be seen in the top half of the hole. This unusual type of crack appeared in the 0.5 mm and in two of the 1 mm diameter holes,

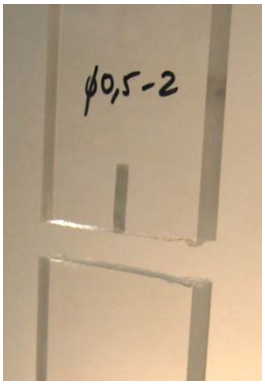

Figure 11. Plate with 0.5 mm diameter hole, after rupture.

In last two columns of Table 1 it can be seen the critical remote load, normalized by the ultimate stress $\frac{\sigma_c^{\infty}}{\sigma_c}$, for the two σ_c obtained from the tensile tests, in order to compare with the FFM predictions. In the latter, plane strain was adopted in calculations, because of the noticeable thickness of the specimens when compared to hole diameters. Three curves were generated by FFM calculations for each σ_c obtained taking different values for K_{Ic} for PMMA material from [8], with the lower, the medium and the higher values (0.8; 1.275 and 1.75 MPa.$\sqrt{m}$). In Figures 12 and 13 comparisons of the experimental results with the FFM predictions can be seen for σ_c=33.8 MPa and σ_c=72.15 MPa, respectively.

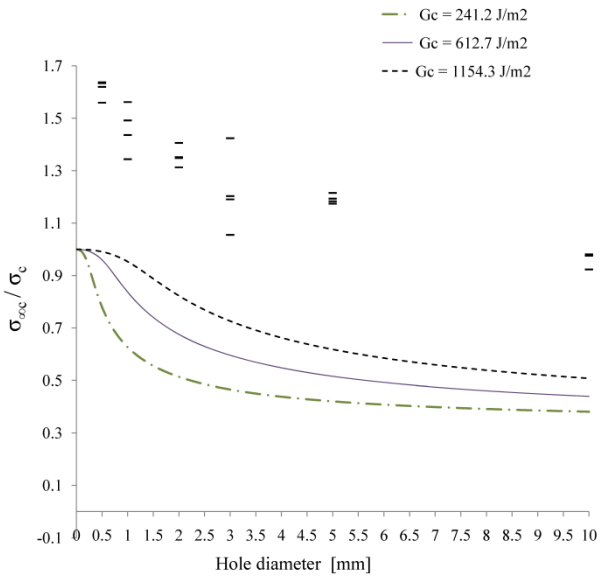

Figure 12. Comparison of the FFM predictions for plate with a hole and of the test results, for σ_c = 33.8 MPa.

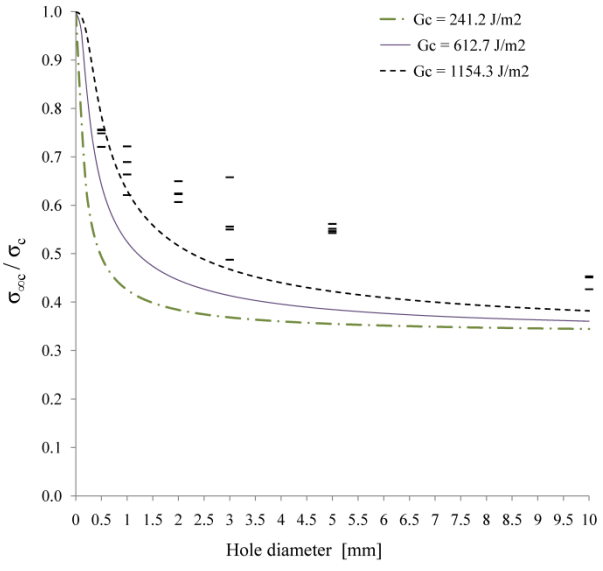

Figure 13. Comparison of the FFM predictions for plate with a hole and of the test results, for σ_c = 73.15 MPa.

4. DISCUSSION AND CONCLUSIONS

Preliminary theoretical and experimental results for characterization of crack onset at circular holes in plates from PMMA subjected to tensile load have been presented. A significant scatter in experimental results, mainly in the plates with small holes has been observed. It appears that PMMA is very sensible to machining and finishing operations and to the existence of fillets, and possibly to heat generation during machining or drilling. Some difficulties were observed in machining some coupons. The mill cutting was not sufficiently smooth. Additionally PMMA has been shown to be clearly sensible to the testing velocities. For example, it is evident in Figure 12 that something is wrong with the ultimate stress, because there are plates with holes supporting much larger tensile stress than plates with no hole. The preliminary results of the Figure 13 show much more reasonable results. It will be important to test plates with holes at a velocity of 5 mm/min and to test CT specimens for K_{Ic} to be able really compare the theoretical predictions by FFM with the experimental results.

REFERENCES

[1] Leguillon, D., *Strength or toughness? A criterion for crack onset at a notch,* European Journal of Mechanics A/Solids, 21, 2002, 61–72.

[2] Mantič, V., *Interface crack onset at a circular cylindrical inclusion under a remote transverse tension. Application of a coupled stress and energy criterion,* International Journal of Solids and Structures 46, 2009, 1287–1304.

[3] Li, J., Zhang, X.B., *A criterion study for non-singular stress concentrations in brittle or quasi-brittle materials*, Engineering Fracture Mechanics 73, 2006, 505–523.

[4] ASTM D638-03. *Standard test method for Tensile Properties of plastic*, ASTM; 2003.

[5] ASTM D5045-99. *Standard test methods for plane-strain fracture toughness and strain energy release rate of plastic materials*, ASTM; 2007.

[6] Souza, J.M.**,** Peres, F. M. and Schön, C.G., *Prática dos Ensaios de Tenacidade à Fratura em Pmma.* Congresso Brasileiro de Engenharia e Ciência dos Materiais – CBECiMat (ref 412-010). 24-28 Nov 2008. Porto de Galinhas, PE, Brasil.

[7] Kim, B.C., Park, S.W., Lee, D.G., *Fracture toughness of the nano-particle reinforced epoxy composite*, Composite Structures 86, 2008, 69–77.

[8] Pilkey, W.D,. *Formulas for Stress, Strain, and Structural Matrices,* Wiley, 1994.